

Electronic supplementary information (ESI)

Improved heat transfer for pyroelectric energy harvesting applications using a thermal conductive network of aluminum nitride in PMN-PMS-PZT ceramics

Qingping Wang^{a,b}, Chris R. Bowen^c, Wen Lei^a, Haibo Zhang^a, Bing Xie^a, Shiyong Qiu^a, Ming-Yu Li^{a,*}, Shenglin Jiang^{a,*}

^a*School of Optical and Electronic Information, Huazhong University of Science and Technology, Wuhan 430074, PR China*

^b*Department of Physics & Mechanical and Electronic Engineering, Hubei University of Education, Wuhan 430205, PR China*

^c*Materials Research Centre, Department of Mechanical Engineering, University of Bath, Claverton Down Road, Bath BA2 7AY, UK*

*Corresponding author: mingyuli.oliver@gmail.com; jslhust@gmail.com.

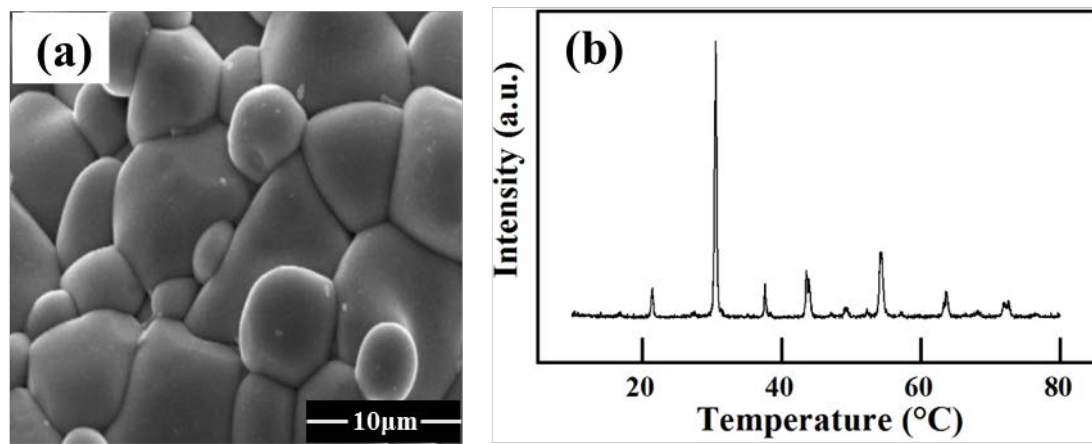


Fig.S1. (a) Scanning electron microscopy (SEM) and (b) X-ray diffraction (XRD) spectrum of the pure PMN-PMS-PZT sample after one-step sintering.

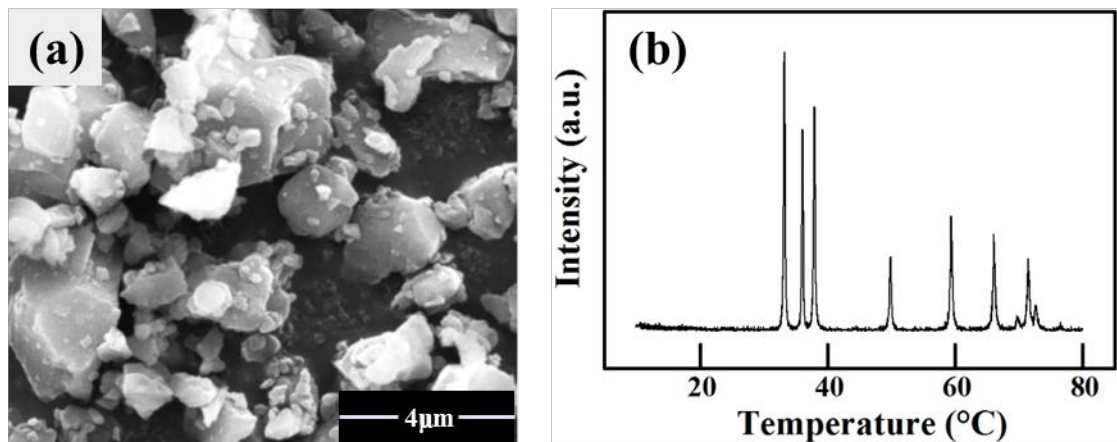


Fig.S2. (a) SEM image and (b) XRD spectrum for the initial AlN power

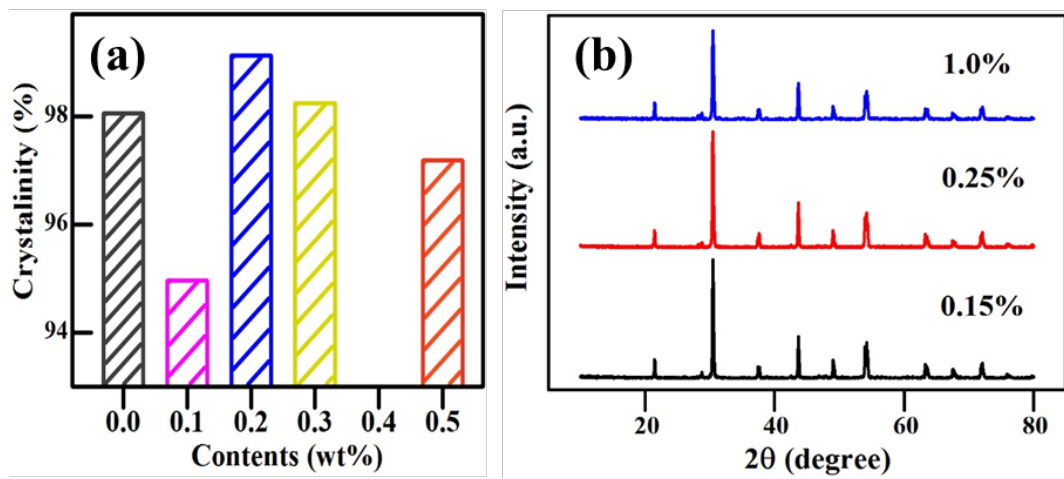


Fig. S3. (a) Crystallinity of the samples with a variation of AlN contents: 0, 0.1, 0.2, 0.3, 0.5 wt.%.

(b) XRD patterns of the samples with various AlN contents: 0.15, 0.25 and 1.0 wt.%.

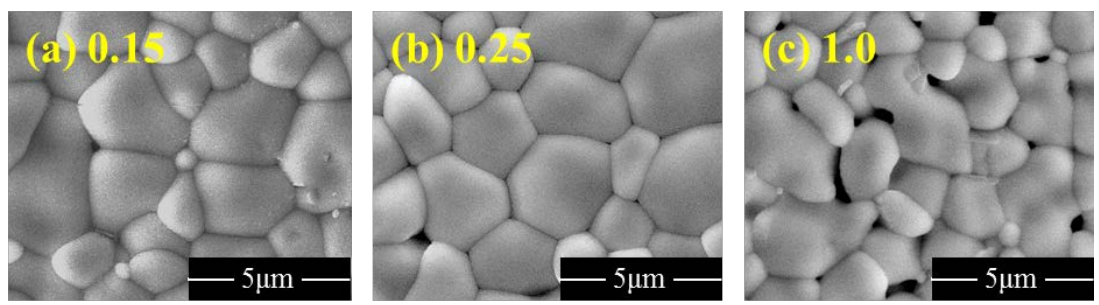


Fig.S4. SEM images of the samples PMN-PMS-PZT: xAlN:(a) $x=0.15$, (b) $x=0.25$, (c) $x=1.0$ wt.%.

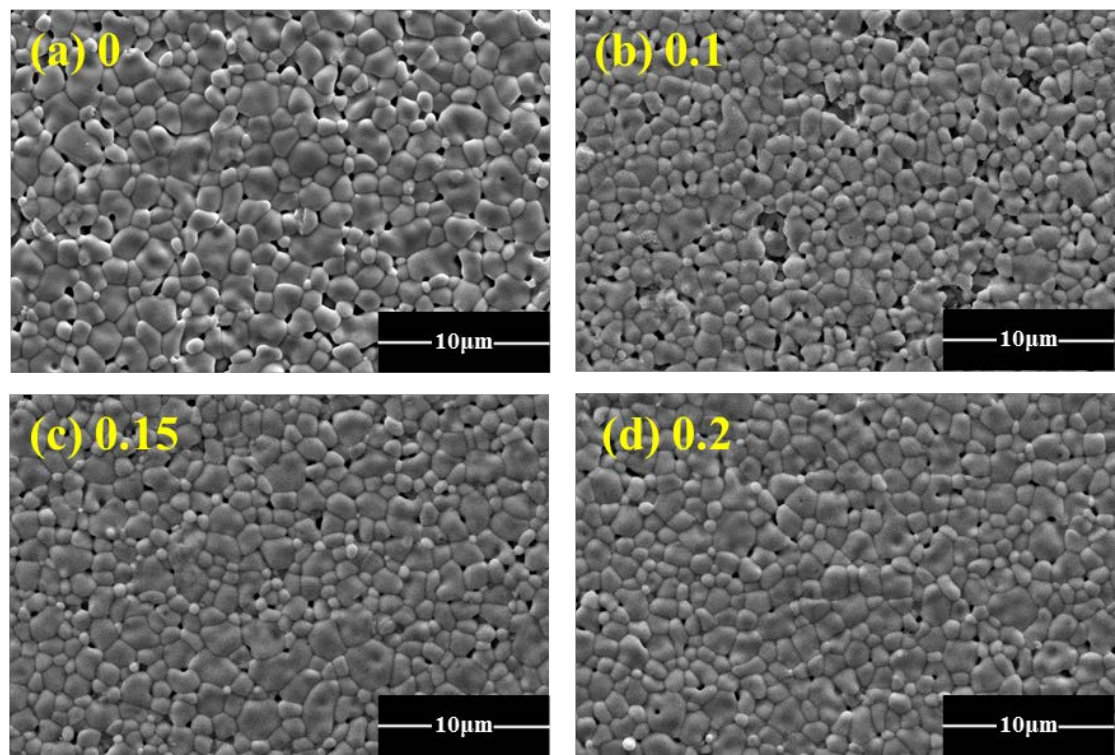


Fig.S5. SEM images of the samples PMN-PMS-PZT: xAlN:(a) $x=0$, (b) $x=0.1$, (c) $x=0.15$, (d) $x=0.2$ wt.%.

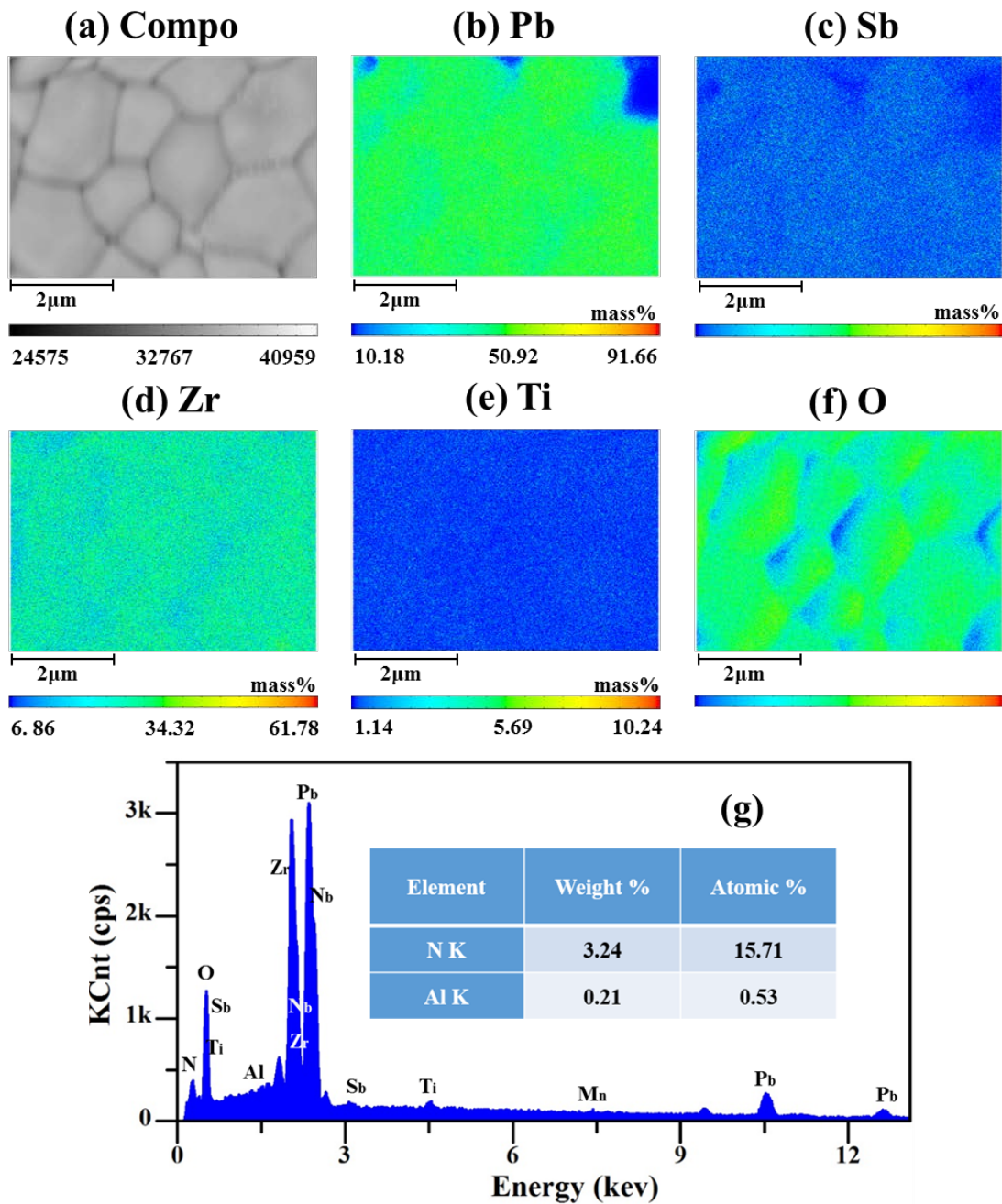


Fig.S6. SEM micrographs of the samples PMN-PMS-PZT: 0AlN. (a) Microstructural image of the composite. Scale bar is 2.0 μ m (b)-(f) the corresponding elemental distribution. (g) The energy-dispersive spectrum of the PMN-PMS-PZT: 0.2AlN sample.

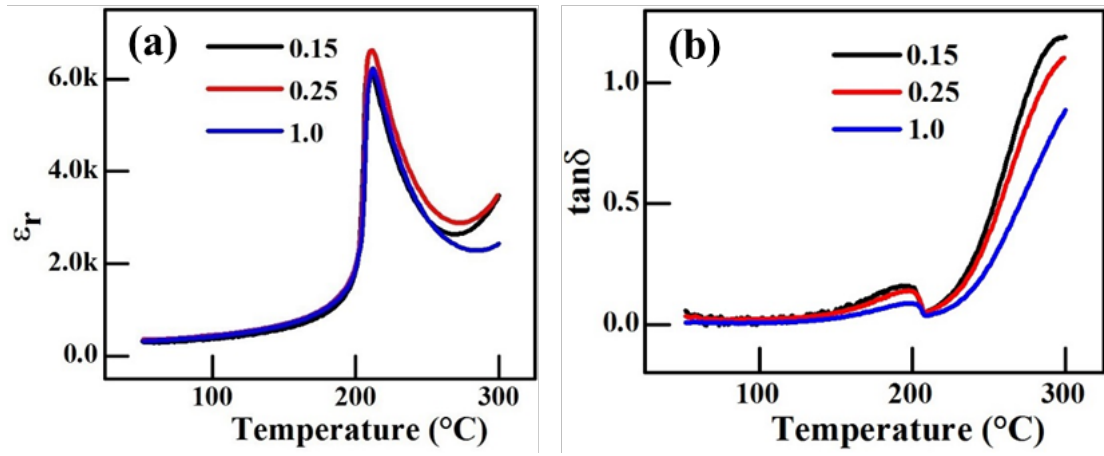


Fig.S7. Temperature-dependent dielectric properties of the materials with various AlN contents: 0.15, 0.25, 1.0 wt.%. (a) Relative permittivity (dielectric constant) and (b) dielectric loss of the corresponding materials at 1 kHz.

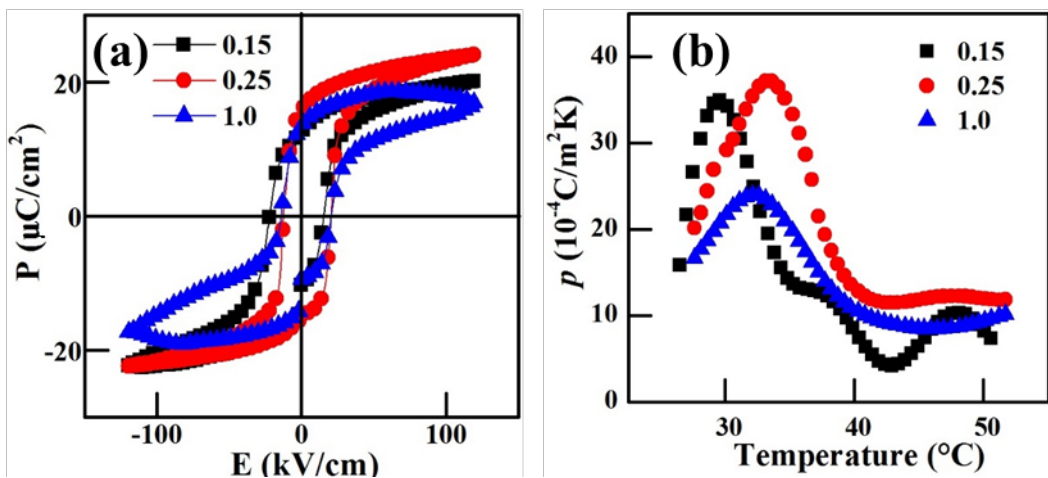


Fig.S8. (a) P-E loops of the samples with various AlN contents: 0.15, 0.25, 1.0 wt.%. (b) Temperature-dependent pyroelectric coefficient of the corresponding samples

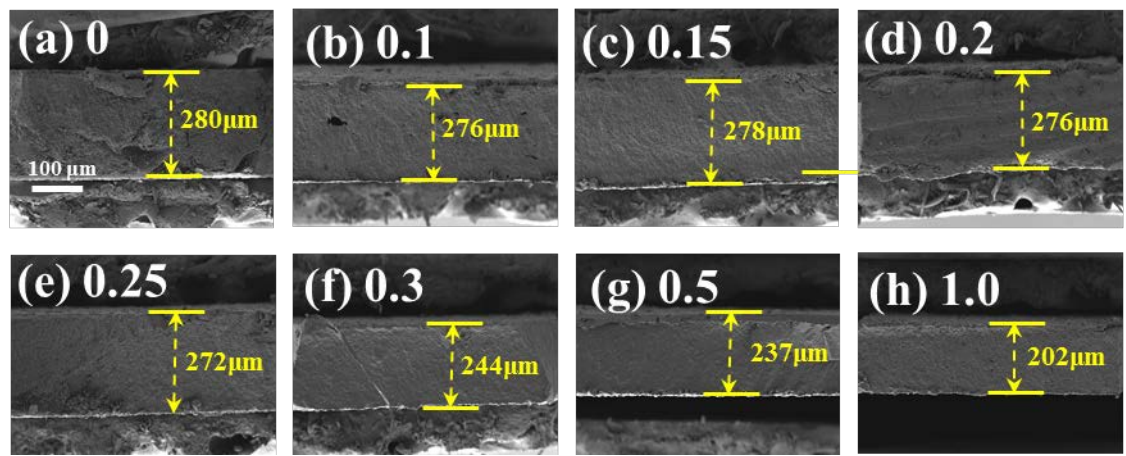


Fig.S9. The thickness of the samples PMN-PMS-PZT: xAlN:(a) x=0, (b) x=0.1, (c) x=0.15,(d) x=0.2, (e) x=0.25, (f) x=0.3, (g) x=0.5, (h) x=1.0 wt.%.

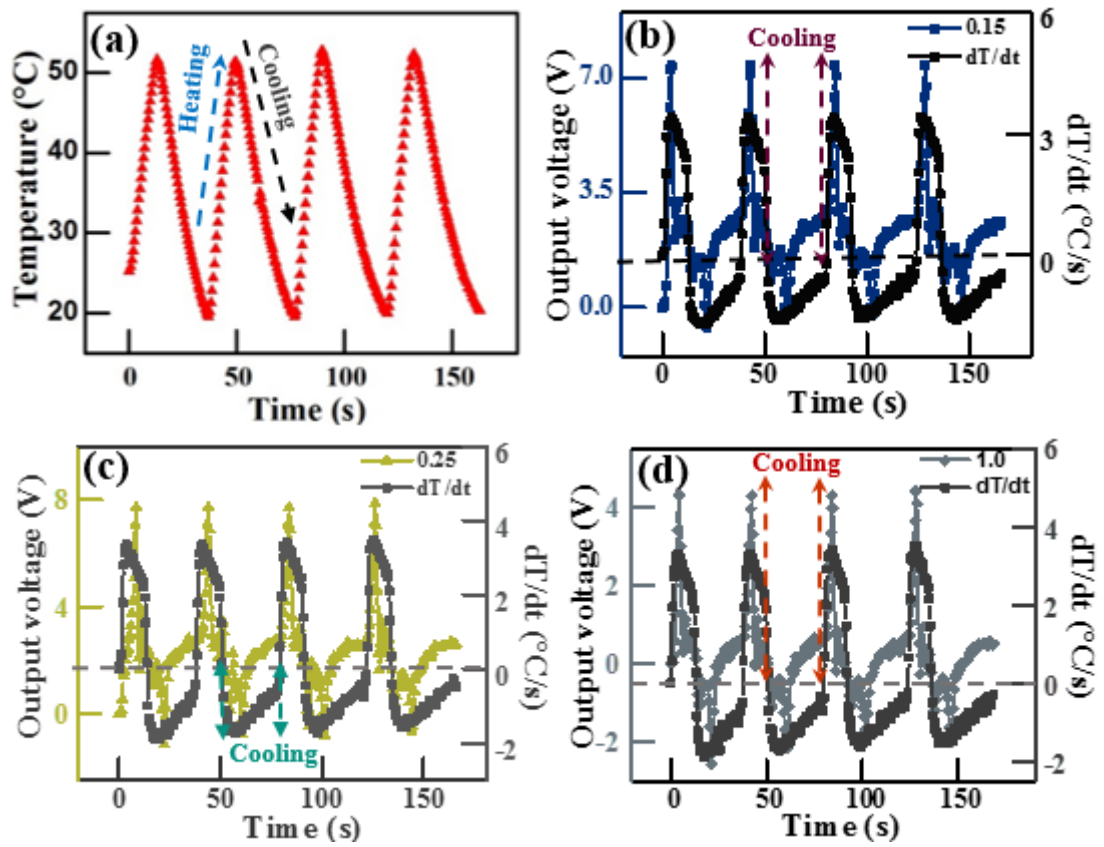


Fig.S10. (a) Temperature variation as a function of time along with corresponding output voltage and rate of temperature change for (b) 0.15 wt.%, (c) 0.25 wt.%, and (d) 1.0 wt.%, respectively, when they are under heating and cooling.

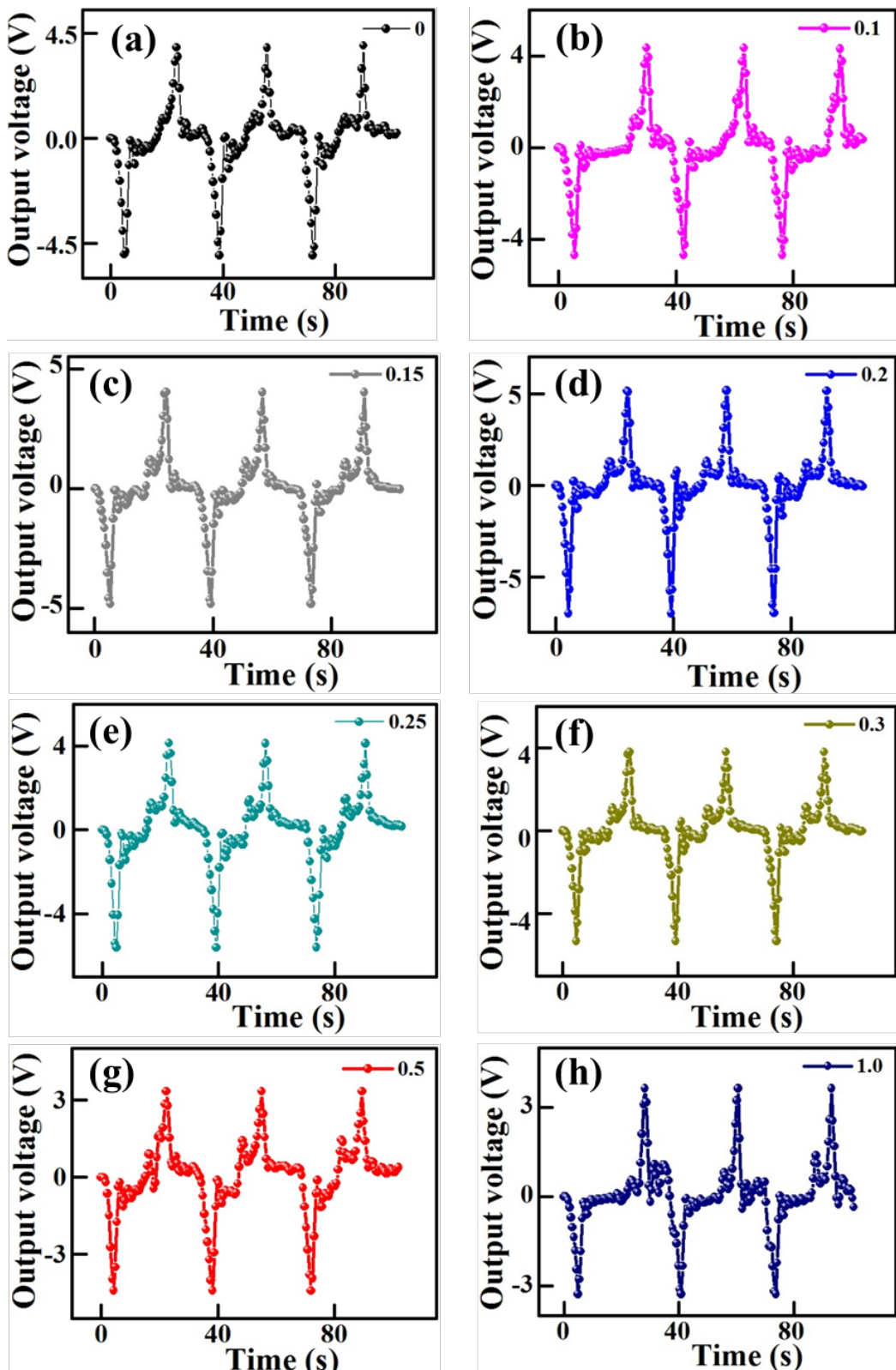


Fig.S11. (a) Output voltage for the samples with 0 wt.% (a), 0.1 wt.% (b), 0.15 wt.% (c), 0.2 wt.% (d), 0.25 wt.% (e) 0.3 wt.% (f), 0.5 wt.%, and 1.0 wt.% AlN contents, respectively, when the two electrodes of pyroelectric devices reversibly connecting to the circuits.

Table 1 Parameters of ceramics with various AlN contents

x (wt.%)	P_r (μC/cm²)	P_s (μC/cm²)	P (10^{-4}C/m²K)	K (W/m°C)
0	13.06	23.90	37.67	0.644
0.1	14.47	20.72	32.49	0.546
0.15	12.57	22.67	34.93	0.662
0.2	16.52	26.59	41.46	0.704
0.25	15.96	24.10	37.25	0.726
0.3	15.06	22.70	33.46	0.612
0.5	9.13	19.21	30.37	0.527
1.0	13.58	16.79	23.98	0.479

Table 2 Energy harvesting parameters for PMN-PMS-PZT: xAlN

x (wt.%)	Output voltage (U_{peak}/V)	Output current ($I_{\text{peak}}/\mu\text{A}$)	Power (μW)	dT/dt (°C/s)
0	7.05	0.705	4.97	3.24
0.10	6.56	0.656	4.30	3.11
0.15	7.35	0.735	5.40	3.38
0.20	8.72	0.872	7.60	3.32
0.25	7.87	0.787	6.19	3.33
0.30	6.21	0.621	3.86	3.21
0.50	5.66	0.566	3.20	3.12
1.0	4.32	0.432	1.86	3.25